MULTITEMPORAL LANDSAT IMAGERY ANALYSIS TO STUDY THE DYNAMICS OF LAND COVER OVER LAKE KIVU REGION

Bikash Basnet and Anthony Vodacek

Center for Imaging Science, Rochester Institute of Technology, Rochester, NY, USA;
bxb6414@rit.edu; vodacek@cis.rit.edu

ABSTRACT

In this study, maximum likelihood supervised classification and post-classification change detection techniques were applied to cloud-free Landsat mosaic scenes formed for three years, 1987, 2001 and 2010, to map land cover changes in the Lake Kivu region in Central Africa. A supervised classification was carried out on the stacked vector of six reflective bands and two vegetation index images for the three years individually with the aid of ground data. Since ground data was not available for 1987, visual interpretation was used to aid supervised classification. The overall seven-class classification accuracies averaged to 77% for the three years. Post-classification change detection technique was used to evaluate land cover change statistics in the region using cross-tabulation. Changes among different land cover classes were accessed. A very severe land cover change has taken place in the region over the past 25 years as a result of human migration and agriculture practices. The major land cover changes in the area include rapid deforestation, urbanization and cropland expansion.

INTRODUCTION

Situated at the center and highest point of the East-African Rift valley, the Lake Kivu region is a biodiversity hotspot. During the nineties, the region faced a number of human tragedies: civil war, genocide, reprisal killings and a massive refugee crisis (1). The displaced people during the conflict found settlement near the shores of Lake Kivu. Since then a large human population around the lake is mounting pressure on the surrounding highland forests for fuel use and subsistence farming, leading to loss of wildlife habitat. The high concentrations of methane and carbon dioxide gases trapped at the bottom of the lake also pose a potential geohazard should the lake overturn. The potential impacts of human-induced environmental stress on the lake system and the geohazard are unknown. A method was therefore needed for examining those human-induced as well as natural land cover changes over time in the region.

Remote sensing imagery provides an efficient means of obtaining information on temporal trends and spatial distribution of land cover since the early days. It also provides a fast, accurate, large-scale, affordable tool for mapping resources and monitoring environmental changes (2). There are numerous ways for approaching the use of remote sensing imagery for determining land use change (3). These change detection methods in the past have been successfully used for land use and land cover study, forest or vegetation change, urban change, environmental changes and many more (4). Change detection is the process of identifying differences in the state of an object or phenomenon by observing it at different times (5). The pre-classification change detection techniques use image differencing, ratios or correlations methods applied to single or multispectral bands, vegetation indices or principal components to obtain “change” vs “no change” maps but they lack information about the nature of change (3). On the other hand, post-classification comparison methods use separate classification of images acquired at different times and quantifies the different types of change between those intervals (6).

This paper describes the methods and results of classifications and post-classification change detection of multitemporal Landsat data of the Lake Kivu region after 1987. The objective of this study is to provide a recent perspective for land cover types and land cover changes that have taken place in the last 25 years in the Lake Kivu region by developing methodology that integrates visual interpretation with supervised classification techniques.

METHODS

Study Area and Data

The Lake Kivu region is situated in Central Africa on the border between Democratic Republic of Congo and Rwanda. The region has a considerable amount of elevation change ranging between 700 m at plains in the north to 4507 m at Mount Karisimbi (7). The region is home to Virunga National Park which consists of two active volcanoes namely Mount Nyiragongo and Mount Nyamuragira (7). Mgahinga national park and Gishwati Forest Reserve are other two preserved forest parks in the region. The average annual rainfall in the region ranges from 1744 mm/yr in Gishwati forests (8) to 2400 mm/yr in high mountains. Despite the proximity of the region to the equator the climate is mild, being moderated by the altitude. There are two dry seasons, a short dry season from January to February and a long dry season from June to September, as well as two wet seasons, one from October to December and the other from March to May. Temperatures depend on altitude and levels of humidity, with Lake Kivu averaging 25°C and high volcanoes at 9.5°C. It extends over 3,214,200 hectares and covers Landsat Worldwide Reference System (WRS-2) Path 173 and Row 61 as shown in Figure 1 (inside oblique box).

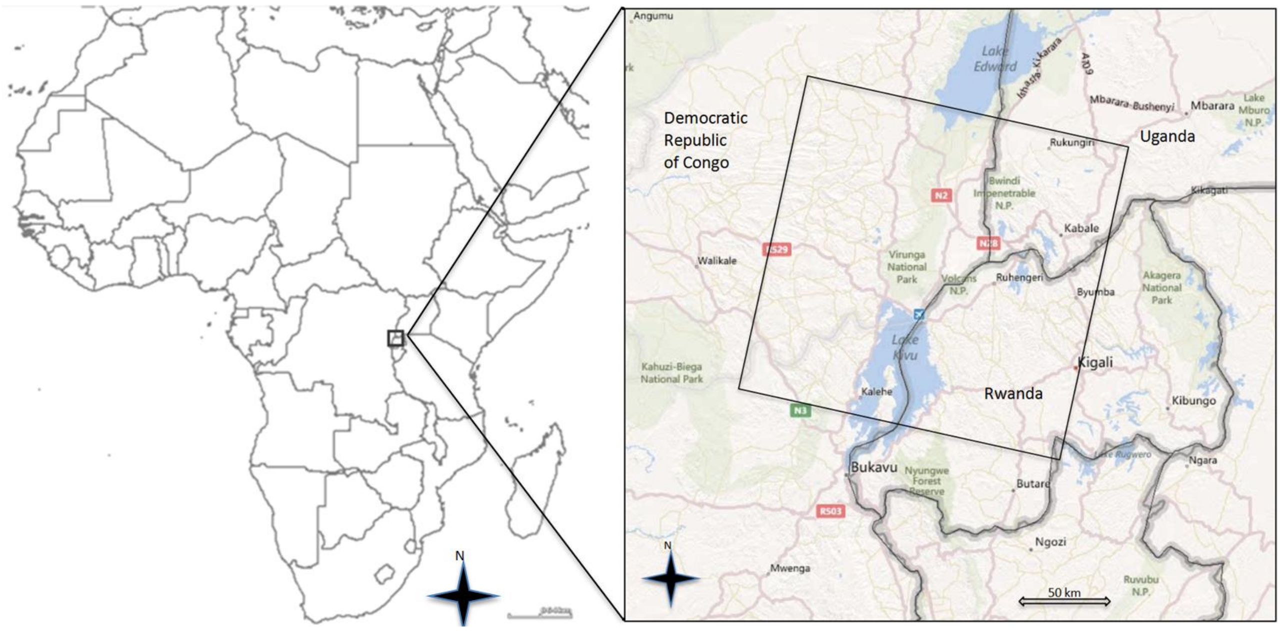

Figure 1. Location of the study area.

The freely available Landsat archive at the United States Geological Survey (USGS) provides the longest-running continuous data set of medium spatial resolution imagery of the Earth, spanning almost four decades. These data provide a unique opportunity to understand deforestation history and land cover dynamics. Available Landsat scenes in the USGS archive for our region of interest were processed using the Landsat Ecosystem Disturbance Adaptive Processing System (LEDAPS) located at the USGS Earth Resources Observation and Science (EROS) Center (9). LEDAPS system produces georeferenced surface reflectance Landsat data products by compensating for atmospheric scattering and absorption effects on the top of atmosphere (TOA) reflectance. It uses the 6S (second simulation of a satellite signal in the solar spectrum) radiative transfer code to compute the transmission, intrinsic reflectance and spherical albedo for relevant atmospheric constituents, including gases, ozone, water vapor and aerosols (10). The processed scenes obtained from EROS were analyzed visually and found to be covered with clouds very frequently, affecting more than half of the data acquisitions. Some significant temporal data gaps were also observed in the imagery collected before 2000. The three most cloud free Landsat images were selected as reference images near each of the years 1990, 2000 and 2010. Table 1 lists those acquisition dates for the images and its sensors. The first objective was to form a cloud free mosaic image for each decade using the reference Landsat scene and its near-date acquisition scenes (maximum 3 in number) and perform land use and land cover change analysis. All the images chosen were limited to dry season months to minimize seasonal effects (11).

Table 1: Date of reference Landsat scenes used in investigation

Date of Imagery	Sensor
August 7, 1987	TM
December 11, 2001	ETM+
September 1, 2010	ETM+

Cloud-free Mosaic formation

The first step in the formation of a cloud-free mosaic was removal of cloud and cloud shadows in all the Landsat scenes used for the study. A composite cloud-shadow mask was formed using a surface reflectance based cloud mask**,** cloud shadow mask and adjacent cloud mask provided as an additional band called quality assurance in the LEDAPS surface reflectance data (9). After the mask was applied to all scenes, a mosaic Landsat image was formed, starting with a reference Landsat scene and then using other selected nearby Landsat images. The final Landsat mosaic image formed near referenced dates 1987, 2001, 2010 were more than 95% cloud free and suitable for land cover change analysis.

Topographic correction

Steep hill and mountain slopes severely affect remote sensing of vegetation. The topographic correction was important in this study as the study area consisted of significant varying topography (4). The Digital Elevation Model (DEM) of the region used was the Advanced Spaceborne Thermal Emission and Reflection Radiometer (ASTER) Global Digital Elevation Model (12). The Landsat image and corresponding DEM image were geo-rectified to UTM zone 35 South, WGS-84 system, before the topographic correction. ENVI software was used to correct the Landsat image for topography.

Land cover classification

The overall objective of the image classification procedure is to automatically categorize all pixels in an image into land cover classes or themes (13). Maximum likelihood classification (MLC) was chosen for this study as it is one of the most common and accurate classifiers that quantitatively evaluates both the variance and covariance of the category spectral response patterns when classifying an unknown pixel (6, 15). It is based on the probability that a pixel belongs to a particular class. The study area was classified into seven main classes: water, forest, agriculture, urban, grassland or pastureland, shrubland and Barren land. Description of these land cover classes are presented in Table 2.

Table 2: Description of different land cover classes of the study area

Class	Description (land use type)
Water	Permanent open water, natural lakes, reservoirs and streams
Forest	Deciduous forest, evergreen forest, mixed forest, woodland and forest plantation with height greater than 5m.
Urban	Residential, commercial services, industrial transportation, built-up land and settlement in villages.
Shrubland	Open general shrubs (Height 0.5-5m). Maybe with scattered herbaceous and sparse trees in between.

Barren Land	Barren areas with no vegetation.
Grassland/ Pastureland	Areas with annual and perennial grasses and pasture areas.
Agriculture	Areas cultivated with annual crops such as vegetable, fruits, tea and bananas.

Different vegetation indexes have been used in the past for improving vegetation classification performance. Lu et al. (14) found a combination of two vegetation indices, TC2 and ND42-57, to be helpful in improving the extraction and separability of pasture, water and urban land covers (see Table 3). These vegetation indices were used in this study to improve the land cover classification performance.

Table 3: Vegetation indexes used in the research.

Vegetation Index	Equation
TC2	−0.285TM1−0.244TM2 − 0.544TM3 + 0.704TM4 + 0.084TM5 − 0.180TM7
ND42_57	(TM4 + TM2 − TM5 − TM7)/(TM4 + TM2 + TM5 + TM7)
Note: TC=tasseled cap transform ND= Normalized difference. The ND number represents the TM spectral band.	

Different training strategies influence the classification map accuracy in the case of the supervised method (15). Around twenty area of interest (AOI) for each class with average size of 10 × 10 pixels were chosen as training data representative of all classes. The locations of the AOI's were chosen using a random stratified method to represent all land cover classes.

A combination of the six reflective bands and two vegetation index images (i.e., stacked vector) was used for the classification of previously formed 1987, 2001 and 2010 Landsat mosaic images. Supervised classification of 2001 and 2010 was done using an Africover land cover map of Rwanda produced by the United Nations Food and Agriculture Organization (FAO) (based on 1999 satellite data) (16). Since no reference ground truth could be obtained for the 1987 image, visual interpretation of the Landsat imagery was used to choose training and test data for supervised classification. An accuracy assessment was carried out using the error matrix for which the literature has provided the meaning of and calculation methods for overall accuracy, producer's accuracy, user's accuracy and kappa coefficient (17). A total of 215 AOI's (different from training data) were used as test samples for accuracy assessment.

Change Detection

After classification of imagery from the individual years was done, a multi-date post-classification comparison change detection algorithm was used to determine changes in the land cover in three intervals, 1987-2001, 2001-2010 and 1987-2010. Post-classification comparison proved to be the effective technique since it provided the nature of change (from-to) between three seven-class thematic maps. ENVI software was used to obtain the change detection results.

RESULTS

The classification maps showing the spatial distribution of land cover for years 1987, 2001 and 2010 is presented in Figure 2. The accuracy assessment of the classification using error matrices are summarized in Table 4. The overall accuracies for 1987, 2001 and 2010 were 76.93%, 78.11% and 76.85%, respectively, with kappa statistics of 70.66%, 72.81% and 71.62%. The shrubland, water and forest had higher accuracies (76-97) % than other classes. The lowest accuracy was of agriculture which could be explained by the fact that it is distributed in a large area and easily misclassified as forests, barren lands and grasslands or pasturelands. The key distinction required in the classification was between forest and non-forested areas. The classification scheme was successful in making this determination.

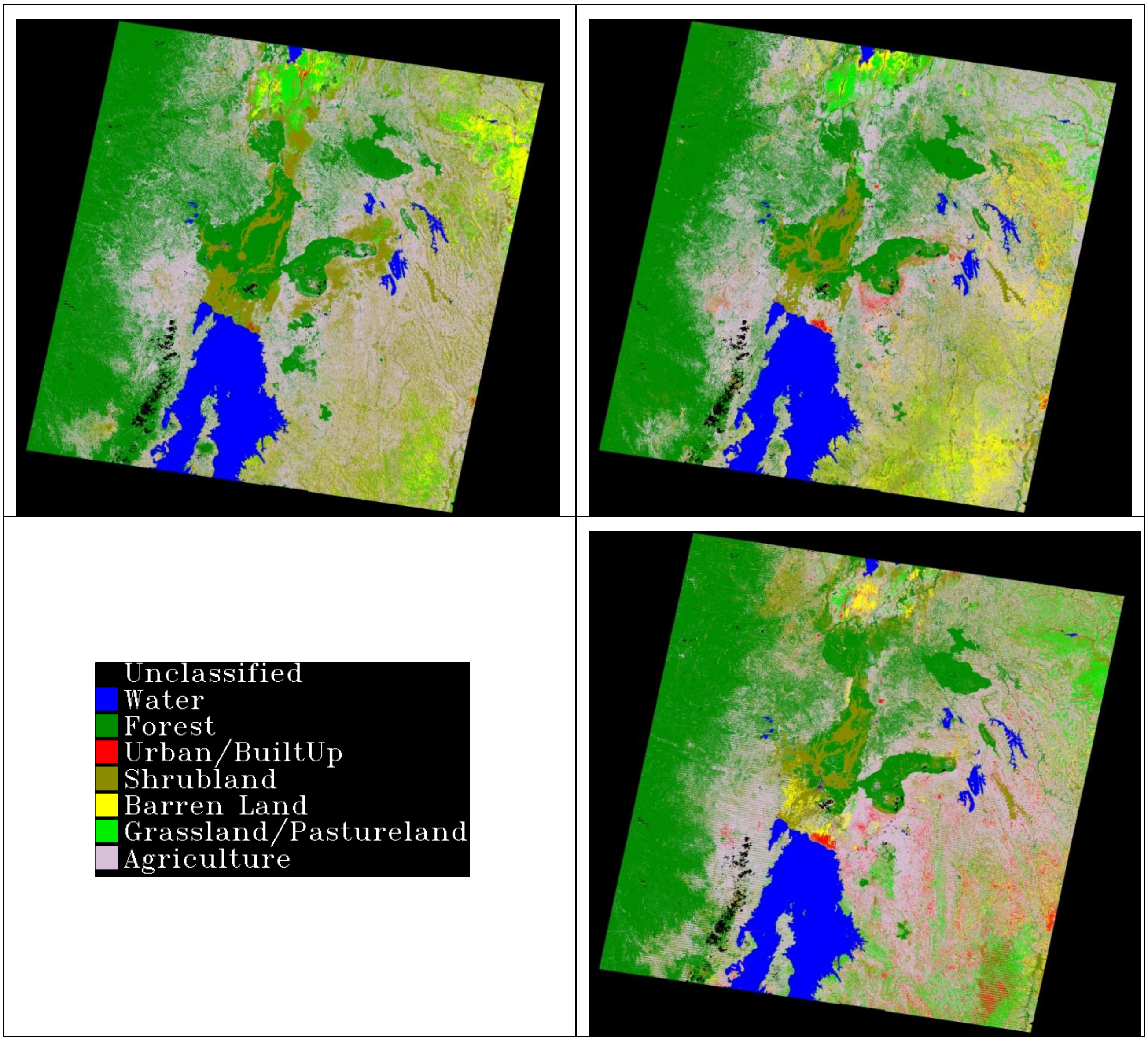

Figure 2. Landsat land cover classifications from 1987 to 2010 for MLC. Clockwise from lower-left, classification legend, thematic maps for 1987, 2001 and 2010.

Table 4: Accuracy statistics for landsat classification results (%).

Land cover class	1987		2001		2010	
	Producer's	User's	Producer's	User's	Producer's	User's
Water	97.82	90.24	99.38	98.35	98.76	98.53
Forest	78.88	99.78	89.99	85.91	90.71	97.74
Urban	65.19	92.47	67.06	79.09	86.84	53.31
Shrubland	82.5	52.73	79.99	78.8	80.65	84.34
Barren Land	90.05	94.9	50.56	33.09	60.53	42.82
Grassland/Pastureland	95.47	78.04	64.6	63.21	29.2	22.13
Agriculture	24.14	34.93	60.91	70.03	56.6	68.67
Overall Accuracy	76.93		78.11		76.85	
Kappa Statistic	70.66		72.81		71.62	

The individual class area and change statistics for the three years are summarized in Table 5. From 1987 to 2010 the urban, agriculture and grassland/pastureland areas increased by approximately 107900 ha, 64700 ha and 68000 ha respectively while water, forest shrubland and barren land areas decreased by 1700 ha, 105300 ha, 94800 ha and 38700 ha respectively. The increase of agriculture areas between 1987 and 2010 can be explained by deforestation, rapid urbanization and population growth in the region. Although the Table 5 suggests forests did not change much between 1987 and 2001, additional change detection studies in the separate regions like Gishwati forest on the Rwanda side confirmed massive deforestation in the area during the nineties, which might have been offset overall by the increase in forest cover in the DPR Congo side of the study area. The migration of people from Congo side to Rwanda due to the conflict might be the reason of increase of forests in the Congo side while deforestation in the Rwanda side.

Table 5: Summary of Landsat classification area statistics for 1987, 2001 and 2010.

Land cover class	1987		2001		2010		Relative change, 1987-2010 (000 ha)
	Area (000 ha)	%	Area (000 ha)	%	Area (000 ha)	%	
Water	221.7	6.9	221.4	6.9	219.9	6.8	-1.7
Forest	1039.6	32.3	1065.0	33.1	934.3	29.1	-105.3
Urban	8.6	0.3	27.9	0.9	116.6	3.6	107.9
Shrubland	585.8	18.2	415.5	12.9	491.0	15.3	-94.8
Barren Land	108.4	3.4	192.7	6.0	69.7	2.2	-38.7
Grassland/Pastureland	114.6	3.6	108.5	3.4	182.6	5.7	68.0
Agriculture	1135.5	35.3	1183.1	36.8	1200.2	37.3	64.7

The matrices of land cover changes from 1987 to 2001, 2001 to 2010 and 1987 to 2010 were created to evaluate the results of land cover conversions. Out of the standing forests of 1,039,600 ha present in 1987, only 718,800 ha of forest were remaining in 2010. This amounts to disappearance of 320,800 ha of standing forest, signifying a massive deforestation in the region over the last 25 years. The majority of the deforested region was converted into cropland and shrubland. However, reforestation efforts in the region seem to be adding forests in the region as shown by conversion of agricultural land into forests in the Table 6. The water areas show the small decreasing trend since 1987 and may be due to change of lake water levels in the region. The urban area increased significantly since 1987 where the shrubland and agriculture area were converted to urban areas. The shrubland located north-west of the city of Goma also diminished in size since 1987. Agriculture, which is the largest land cover class in the region, was shown to be flourishing for the last 25 years as seen by its figures in the Table 6. The migration of refugees after the civil war in 1994 and rapid deforestation are the prime reason for its expansion. Barren lands were found to be reduced in size from 1987 to 2010 while grasslands were found to go through expansion over the same time. The low classification accuracy of barren lands, grasslands or pasturelands and agriculture, however, cast some shadows on the trends they are showing in the region. Some seasonal changes might have also affected our results as lack of more cloud-free data hindered us from removing those effects completely from our analysis.

Table 6: Matrices for land cover and changes (000 ha) from 1987 to 2010

a. 1987-2001								
2001	1987							2001 Total
	Water	Forest	Urban/B	Shrubland	Barren Land	Grassland /Pasture	Agriculture	
Water	219.7	0.3	0.1	0.9	0.1	0.0	0.2	221.4
Forest	0.5	788.4	0.3	45.7	1.2	2.6	226.3	1,065.0
Urban/Builtup	0.0	2.2	0.8	10.7	0.9	1.6	11.7	27.9
Shrubland	1.2	57.2	2.0	159.0	16.1	16.6	163.4	415.5
Barren Land	0.0	4.8	1.9	65.6	29.4	22.0	69.0	192.7
Grassland/P	0.0	1.5	1.3	32.6	26.1	25.4	21.6	108.5
Agriculture	0.1	185.2	2.2	271.3	34.6	46.4	643.3	1,183.1
1987 Total	221.7	1,039.6	8.6	585.8	108.4	114.6	1,135.5	3,214.2
b. 2001-2010								
2010	2001							2010 Total
	Water	Forest	Urban/B	Shrubland	Barren Land	Grassland /Pasture	Agriculture	
Water	218.0	0.5	0.0	1.3	0.0	0.0	0.1	219.9
Forest	0.3	742.7	1.0	31.7	2.6	1.1	154.8	934.3
Urban/Builtup	0.0	3.3	5.1	21.2	30.0	6.4	50.5	116.6
Shrubland	1.7	100.7	3.5	128.3	17.5	22.8	216.4	491.0
Barren Land	0.0	3.1	2.1	19.3	10.5	8.2	26.4	69.7
Grassland/P	0.0	4.7	1.5	34.1	38.3	29.9	74.1	182.6
Agriculture	1.3	209.9	14.7	179.7	93.7	40.2	660.7	1,200.2
2001 Total	221.4	1,065.0	27.9	415.5	192.7	108.5	1,183.1	3,214.2
c. 1987-2010								
2010	1987							2010 Total
	Water	Forest	Urban/B	Shrubland	Barren Land	Grassland /Pasture	Agriculture	
Water	218.2	0.5	0.1	1.0	0.0	0.0	0.1	219.9
Forest	0.6	718.8	0.3	37.6	1.0	4.2	171.7	934.3
Urban/Builtup	0.0	3.1	1.3	39.9	11.0	8.9	52.3	116.6
Shrubland	1.7	118.5	1.7	137.1	17.6	22.7	191.6	491.0
Barren Land	0.1	4.0	0.7	28.0	3.9	9.2	23.7	69.7
Grassland/P	0.0	5.4	0.9	57.3	41.2	24.7	53.1	182.6
Agriculture	1.1	189.3	3.6	284.9	33.8	44.8	642.8	1,200.2
1987 Total	221.7	1,039.6	8.6	585.8	108.4	114.6	1,135.5	3,214.2

CONCLUSIONS

The objective of this study was to provide a recent perspective on land cover types and land cover changes that have taken place in the Lake Kivu region over past 25 years. This was done by producing landscape change maps and statistics after supervised classifications of cloud-free Landsat mosaic scenes for the years 1987, 2001 and 2010. The results quantify the land cover change pattern in the region and demonstrate the potential of multitemporal Landsat data to provide economical means to map and analyze land cover over time. The study area was found to have undergone severe land cover change as a result of human migration (presumably the displaced people) after the civil war, population growth and subsistence farming. Deforestation was the major land cover change in the region along with urbanization and cropland expansion. Reforestation efforts were also done over time but it was not enough to balance deforestation. The future work would be to expand these results by developing methods to access data previously avoided due to larger cloud cover fractions.

ACKNOWLEDGEMENTS

This project was funded by the John D. and Catherine T. MacArthur Foundation and the National Science Foundation (IIP-0917839).

REFERENCES

1 Verpoorten M, 2012. Detecting hidden violence: The spatial distribution of excess mortality in Rwanda. Political Geography, 31(1): 44-56

2 Rogan J & D Chen, 2004. Remote sensing technology for mapping and monitoring land-cover and land-use change. Progress in Planning, 61: 301-325

3 Yuan F, K E Sawaya, B C Loeffelholz, & M E Bauer, 2005. Land cover classification and change analysis of the Twin Cities (Minnesota) Metropolitan Area by multitemporal Landsat remote sensing. Remote Sensing of Environment, 98, no. 2-3: 317-328

4 Lu D, P Mausel, E Brondizios & E Moran, 2004. Change detection techniques. International Journal of Remote Sensing, 25(12): 2365–407

5 Singh A, 1989. Digital change detection techniques using remotely-sensed data. International Journal of Remote Sensing, 10(6): 989–1003

6 Shalaby A & R Tateishi, 2007. Remote sensing and GIS for mapping and monitoring land cover and land-use changes in the Northwestern coastal zone of Egypt. Applied Geography, 27 (1), pp. 28-41

7 MacKay, M E, S K Rowland, PJ Mouginis-Mark, & H Garbeil, 1999. Thick lava flows of Karisimbi volcano, Rwanda: Insights from SIR-C interferometric topography. Bulletin Volcanology, **60**: 239 – 251

8 Sun C, B A Kaplin; K A Kristensen, V Munyaligoga, J Mvukiyumwami, K K Kajondo & T C Moermond, 1996. Tree Phenology in a Tropical Montane Forest in Rwanda. Biotropica, 28(4):668-681

9 Masek, J G, E F Vermote, N Saleous, R Wolfe, F G Hall,K F Huemmrich, F Gao, J Kutler & T K Lim, 2006. A Landsat surface reflectance data set for North America, 1990-2000. Geoscience and Remote Sensing Letters, 3: 68-72

10 Vermote E F, D. Tanre, J L Deuze, M Herman & J J Morcrette, 1997. Second simulation of the satellite signal in the solar spectrum, 6S: An overview. IEEE Transactions on Geoscience and Remote Sensing, 35: 675–86

11 Maingi J K & S E Marsh, 2001. Assessment of environmental impacts of river basin development on the riverine forests of eastern Kenya using multi-temporal satellite data. International Journal of Remote Sensing, 22(14): 2701-2729

12 National Aeronautics and Space Administration, NASA's Earth Observing System Data and Information System. http://reverb.echo.nasa.gov/reverb/#utf8=%E2%9C%93&spatial_map= satellite & spatial_type = rectangle (last date accessed: 1 May, 2012)

13 Lillesand T M & R W Kiefer, 2000. Remote Sensing and Image Interpretation (John Wiley & Sons Inc Press). 4th edition, 724 pp

14 Lu D, Q Weng, E Moran, G Li & S Hetrick, 2011. Remote Sensing Image Classification. In Weng Q : Advances in Environmental Remote Sensing: Sensors, Algorithms, and Applications, (CRC Press/Taylor and Francis), chapter 9, 223-243

15 Stow D A, & D M Chen, 2002. Sensitivity of multitemporal NOAA AVHRR data of an urbanizing region to land-use/land-cover change and misregistration. Remote Sensing of Environment, 80(2): 297-307

16 Food and Agriculture Organization of the United Nations, Multipurpose Africover Databases on Environmental resources (MADE) available for 19 countries. http://www.africover.org (last date accessed: 10 May 2012)

17 Congalton R G, 1991. A review of assessing the accuracy of classification of remotely sensed data. Remote Sensing of Environment, 37: 35